Geophysical Research Letters

RESEARCH LETTER
10.1029/2023GL103099

Key Points:

- Equilibrium between variance production and dissipation is a requirement for good performance of Monin-Obukhov Similarity Theory (MOST)
- Fluxes estimated by MOST are more uncertain when the flux magnitudes are small and when variance transport or storage are high
- The relaxed eddy accumulation method can still yield robust flux estimates even when MOST models underperform

Supporting Information:

Supporting Information may be found in the online version of this article.

Correspondence to:

E. Bou-Zeid,
ebouzeid@princeton.edu

Citation:

Zahn, E., Bou-Zeid, E., & Dias, N. L. (2023). Relaxed eddy accumulation outperforms Monin-Obukhov flux models under non-Ideal conditions. *Geophysical Research Letters*, *50*, e2023GL103099. https://doi.org/10.1029/2023GL103099

Received 31 JAN 2023
Accepted 13 MAR 2023

Author Contributions:

Conceptualization: Einara Zahn, Elie Bou-Zeid, Nelson Luís Dias
Data curation: Einara Zahn
Formal analysis: Einara Zahn, Elie Bou-Zeid, Nelson Luís Dias
Investigation: Einara Zahn, Elie Bou-Zeid, Nelson Luís Dias
Methodology: Einara Zahn, Elie Bou-Zeid, Nelson Luís Dias
Resources: Elie Bou-Zeid
Supervision: Elie Bou-Zeid
Writing – original draft: Einara Zahn, Elie Bou-Zeid, Nelson Luís Dias

Relaxed Eddy Accumulation Outperforms Monin-Obukhov Flux Models Under Non-Ideal Conditions

Einara Zahn[1], Elie Bou-Zeid[1], and Nelson Luís Dias[2]

[1]Department of Civil and Environmental Engineering, Princeton University, Princeton, NJ, USA, [2]Department of Environmental Engineering, Federal University of Paraná, Curitiba, Brazil

Abstract The Monin-Obukhov Similarity Theory (MOST) links turbulent statistics to surface fluxes through universal functions. Here, we investigate its performance over a large lake, where none of its assumptions (flat homogeneous surface) are obviously violated. We probe the connection between the variance budget terms and departure from the nondimensional flux-variance function for CO_2, water vapor, and temperature. Our results indicate that both the variance storage and its vertical transport affect MOST, and these terms are most significant when small fluxes and near neutral conditions were prevalent. Such conditions are common over lakes and oceans, especially for CO_2, underlining the limitation of using any MOST-based methods to compute small fluxes. We further show that the relaxed eddy accumulation (REA) method is more robust and less sensitive to storage and transport, adequately reproducing the eddy-covariance fluxes even for the smallest flux magnitudes. Therefore, we recommend REA over MOST methods for trace-gas flux estimation.

Plain Language Summary The Monin-Obukhov Similarity Theory (MOST) is a cornerstone of Earth observations and models. It defines a set of functions that are commonly used to estimate the exchange of heat, water vapor, and other trace gases between the surface and the atmosphere. MOST was originally formulated for "ideal" conditions that rarely prevail in the real world (e.g., fair steady weather and large flat surfaces with little spatial variation in surface cover or moisture conditions). Here, we show that the theory may be equally inaccurate under supposedly ideal conditions where its assumptions are met. We investigate the performance of MOST above a large lake, identifying additional constraints on its performance related to the behavior of turbulence in the atmosphere. One consequential finding is that the theory misrepresents the exchange of small fluxes, which are prevalent over lakes and oceans. In our analyses, it predicted high CO_2 fluxes from the lake when in reality the fluxes were very small, a problem that can hinder the understanding of the global carbon cycle. We show that the relaxed eddy accumulation method, an alternative to MOST, not only outperforms, but is also more robust to deviations from ideal conditions, representing small fluxes more accurately.

1. Introduction

Since its inception almost 70 years ago (Monin & Obukhov, 1954), the validity of the Monin-Obukhov Similarity Theory (MOST) has been investigated across a range of sites, with mixed results, above both flat and complex terrains (Asanuma & Brutsaert, 1999; Barskov et al., 2019; Cancelli et al., 2012; Chor et al., 2017; Dellwik & Jensen, 2005; Denmead & Bradley, 1985; Detto et al., 2008; Dyer, 1974; Dyer & Hicks, 1970; Hogstrom, 1988; Hsieh et al., 2008; Katul et al., 1995; Katul, Hsieh, et al., 1996; Li et al., 2012; Raupach, 1979; Waterman et al., 2022; Weaver, 1990; Williams et al., 2007; Zahn, Dias, et al., 2016). Nonetheless, despite its known limitations, MOST functions—in particular the flux-gradient relation—have been directly or indirectly implemented to estimate scalar fluxes in field measurements or as surface parameterization schemes in large scale models. The variance function has also been used in closure parameterizations in Earth System Models that implement high-order schemes (Waterman et al., 2022). Furthermore, the variance method has been used in gap-filling methods (Cava et al., 2008; Dias et al., 2009). Alternatives and adjustments to MOST have been proposed, but none seems to be able to compete with the elegant simplicity and breadth of applicability of the original theory. As a consequence, studies focused on advancing MOST implementation, delineating its skill limits, or proposing alternative formulations continue to be of great relevance to the various geoscientific research communities.

Writing – review & editing: Einara Zahn, Elie Bou-Zeid, Nelson Luís Dias

According to Foken (2006), the ideal conditions for implementation of MOST are (a) measurement heights z limited to the surface layer ($z \lessapprox 3$ h, where h is the canopy height), (b) stability range $|\zeta| \leq 1$–2 (where $\zeta = z/L$ is the MOST stability parameter and L is the Obukhov length), and (c) homogeneous surfaces. Under typical waves conditions (no swell or breaking waves), lakes are surfaces that satisfy most of these requirements, in particular the homogeneity of sources of water vapor, temperature, and CO_2. However, as will be discussed in our study, even under these conditions, deviations from MOST are observed. To date, few studies have focused on such assessments of MOST, or alternative flux models such as the relaxed eddy accumulation (REA) method, over water surfaces (Armani et al., 2020; Assouline et al., 2008; Cancelli et al., 2012; Dias & Vissotto, 2017), while even fewer investigated the performance of MOST functions to compute CO_2 fluxes above freshwater bodies (Xiao et al., 2014; Zhao et al., 2019) or oceans (Iwata et al., 2004; Lammert & Ament, 2015). Nevertheless, these micrometeorological methods offer a direct approach to estimate air-sea gas exchange that circumvents the need for estimating a transfer velocity (Zemmelink et al., 2004).

To help bridge these knowledge gaps, this study explores the turbulence dynamics responsible for modulating MOST performance. We first investigate the performance of the variance method for water vapor, temperature, and CO_2 at four levels above lake Geneva, in Switzerland. The departure from MOST is then further explored based on the different terms of the variance budget, and implications to other similarity functions are discussed. Multiple measurement levels are rarely available in such experiments, but are needed to directly compute the budget terms we rely on in the present analyses. Given the limitations of MOST, we then investigate whether the REA method—which is similar in formulation to the variance method but does not rely on an empirical MOST function or stability parameter—is more robust to the estimation of low fluxes. The questions that motivate this study are the following

1. What physical processes, and corresponding terms in the variance budget, explain deviations from MOST?
2. Does the REA method suffer from the same limitations as the variance and flux-gradient methods?

To answer these questions, we demonstrate the impacts of the variance budget terms, with emphasis on vertical transport and storage of variance, on the deviation from MOST. We then conclude with a comparison of fluxes for all three scalars above the lake using eddy-covariance, variance function, and the REA methods, explaining why the REA performance is superior to MOST-based approaches.

2. Theory

2.1. Variance Budget of Scalars

Assuming horizontal homogeneity, the variance budget for a scalar s can be written as (Stull, 1988):

$$\underbrace{\frac{\partial \overline{s'^2}}{\partial t}}_{S_s} = \underbrace{-2\overline{w's'}\frac{\partial \overline{s}}{\partial z}}_{P_s} \underbrace{-\frac{\partial \overline{(w's's')}}{\partial z}}_{T_s} \underbrace{-2\epsilon_s}_{D_s}, \tag{1}$$

where $\overline{\mu}$ represents the mean estimated from a time average of a statistic μ, μ' is the turbulent fluctuation from the mean $\left(\mu' = \mu - \overline{\mu}\right)$; t is time; and z and w are the vertical coordinate and velocity component, respectively. The different budget terms are S_s, the local storage of variance; P_s, the gradient production term; T_s, the vertical turbulent transport; and D_s, the molecular dissipation of variance. The radiative term in the variance budget for temperature was neglected. Note that the negative signs were already included in the definition of each term. All terms are further nondimensionalized by an "estimate" of production P_s^* obtained using attached eddy hypothesis scaling $\frac{\partial \overline{s}}{\partial z} \approx \frac{s_*}{\kappa z}$ and computed as

$$P_s^* = \frac{u_* s_*^2}{\kappa z}, \tag{2}$$

where κ is the von Karman constant, $u_* = \left(\overline{w'u'}^2 + \overline{w'v'}^2\right)^{1/4}$ is the friction velocity, and $s_* = \overline{w's'}/u_*$ is the turbulent scale for s. Our analyses will thus investigate the importance of each term with respect to production.

2.2. Monin-Obukhov Nondimensional Functions for Variance and Gradients

MOST postulates the existence of nondimensional universal functions valid for any scalar (Foken, 2017). According to the theory, these functions are solely governed by the Obukhov stability parameter ζ,

$$\zeta = -\frac{\kappa z g \overline{w'T_v'}}{u_*^3 \overline{T_v}}, \tag{3}$$

where g is gravity and T_v is the virtual temperature. By definition, $\zeta > 0$ for stable conditions, $\zeta \approx 0$ for near neutral conditions, and $\zeta < 0$ for unstable conditions.

Two well explored MOST non-dimensional functions are the gradient function $\Psi_s(\zeta)$ and the variance function $\phi_s(\zeta)$, defined as

$$\Psi_s(\zeta) = \frac{\partial \overline{s}}{\partial z}\frac{\kappa z}{s_*}, \tag{4}$$

$$\phi_s(\zeta) = \sigma_s / s_*, \tag{5}$$

where $\sigma_s = \left(\overline{s'^2}\right)^{1/2}$ is the standard deviation of s'. The most commonly used empirical forms of these functions are (Hogstrom, 1988; Kaimal & Finnigan, 1994).

$$\Psi_s(\zeta) = C_1(1 - C_2\zeta)^{-1/2}, \tag{6}$$

$$\phi_s(\zeta) = C_3(C_4 - \zeta)^{-1/3}, \tag{7}$$

where C_1, C_2, C_3, and C_4 are empirical parameters obtained from field (Businger et al., 1971; De Bruin et al., 1993; Hogstrom, 1988; Kaimal & Finnigan, 1994; Liu et al., 1998; Wyngaard et al., 1971) or numerical experiments (Maronga & Reuder, 2017). These functions connect the gradient or the variance of a scalar to its fluxes (represented by s_*). If the universality hypothesized by MOST is valid, Ψ_s (and ϕ_s) should be equal for any scalar (Hill, 1989). This is the most important feature of the theory since it provides a tool to compute fluxes of a scalar solely from its gradient or variance, which can be obtained using slower or cheaper/simpler sensors (e.g., thermocouples or capacitance hygrometers) or from fast gas sensors without a sonic anemometer. This relaxes the need for fast velocity measurements or careful sensor position or distortion corrections (Katul et al., 1994; Katul, Finkelstein, et al., 1996).

Similarly, in Earth System or numerical prediction models, Equation 6 is used to estimate the flux exchange between the surface and atmosphere. Explicitly, turbulent fluxes from the flux-gradient method (FG) and from the flux-variance method can be computed as follows:

$$\overline{w's'}_{FG} = u_* \frac{\partial \overline{s}}{\partial z}\frac{\kappa z}{\Psi_s(\zeta)}, \tag{8}$$

$$\overline{w's'}_{FV} = u_* \frac{\sigma_s}{\phi_s(\zeta)}. \tag{9}$$

Both equations can be further manipulated by combination with expressions 3, 6, and 7. Depending on the available data, the fluxes might be found using an iterative process (such as when u_* is not available) or directly when u_* is measured or when measurements for "proxy" scalars, assumed to be similar to the scalar of interest, are available.

2.3. Relaxed Eddy Accumulation

The REA method (Businger & Oncley, 1990) can be derived directly from the eddy-covariance expression, after assuming linearity between w' and s' (Katul, Finkelstein, et al., 1996; Katul et al., 2018). The derivation of REA is shown Section S1 in Supporting Information S1, where the final flux expression is

$$\overline{w's'}_{\mathrm{REA}} = \beta_s \sigma_w \left(\overline{s^+} - \overline{s^-}\right). \tag{10}$$

β_s is an empirical coefficient, σ_w is the standard deviation of the vertical velocity, and $\Delta s = \overline{s^+} - \overline{s^-}$ is the difference in concentration s for updrafts ($\overline{s^+}$, including only measurements of s when $w' > 0$) and downdrafts ($\overline{s^-}$, including only measurements when $w' < 0$).

While the coefficient β_s was originally proposed to be similar across scalars but a function of the stability parameter, many studies found no clear variability with ζ (Businger & Oncley, 1990; Katul, Finkelstein, et al., 1996; Zahn, Dias, et al., 2016). In fact, various studies show that β_s is quite steady with an average of ≈0.6 (Bowling

et al., 1998; Katul, Finkelstein, et al., 1996) for different scalars, suggesting that the coefficient computed for a "proxy" scalar can be extrapolated to other scalars.

Field implementations of REA usually consist of two separate containers sampling air for updrafts and downdrafts in order to compute $\Delta s = \overline{s^+} - \overline{s^-}$ (Bowling et al., 1998). According to Katul, Finkelstein, et al. (1996), because only the accumulation measurements are required (not instantaneous correlations), slow response sensors can be employed. Bowling et al. (1998) argues that REA might be even more appropriate than conventional EC systems for measuring small CO_2 fluxes over the ocean. According to the authors, EC sensors might lack the sensitivity to measure the concentrations when CO_2 fluxes are very small. REA, on the other hand, allows measuring the concentration from larger air samples and more accurate analysis with high-precision techniques. Thus, the REA method is a very popular alternative to measure trace gases when measurements by eddy-covariance systems are expensive or not possible.

3. Experimental Data

3.1. Site Details

The data set used in our analyses is from the Lake-Atmosphere Turbulent Exchange field campaign (August–October 2006) over Lake Geneva, Switzerland (details of the experiment can be found in Bou-Zeid et al. (2008) and Vercauteren et al. (2008)). Eddy-covariance data was sampled at four levels above the water surface ($z = 1.65$, 2.30, 2.95, and 3.60 m) at 20 Hz. All levels were equipped with a sonic anemometer (Campbell Scientific CSAT3) and open-path gas analyzer (Licor-7500), which simultaneously collected time series of CO_2 (c), water vapor (q), atmospheric pressure (P), sonic temperature (T_s), and the velocity components in the streamwise (u), cross-stream (v), and vertical (w) directions. Only unstable conditions were considered.

3.2. Data Processing

Quality control of the raw high-frequency data included removal of periods identified by various sensors flags, detection and removal of outliers, and gap-filling (Zahn, Chor, & Dias, 2016). Pre-processing consisted of density corrections for c and q (Detto & Katul, 2007) and double rotation of the velocity components. The turbulent fluctuations were computed around the 30-min average. In addition, a stationarity statistic for variances was computed based on the test described in Foken (2017),

$$\xi_s = \left| \frac{\overline{s's'}_{5\,\mathrm{min}} - \overline{s's'}_{30\,\mathrm{min}}}{\overline{s's'}_{30\,\mathrm{min}}} \right| \times 100, \tag{11}$$

who suggested that steady-state conditions can be assumed if $\xi_s < 30\%$. We did not discard data based on this criterion; instead, ξ_s is used solely for the purpose of investigating how nonstationarity impacts the variance function. Nonetheless, we restricted our data according to the wind direction, selecting only periods when the angle between the mean wind and the sensor axis was smaller than 135°.

We verified the existence of a time-varying sensor mean bias for scalars in our data set, which prevented the accurate computation of mean scalar gradients. For this reason, the flux-gradient expression 6 was here estimated from the residual of the variance budget equation ($P_s = S_s - T_s - D_s$) assuming that the effects of horizontal advection are small, which was confirmed by Assouline et al. (2008) for this data set. Note that the transport term is solely based on turbulent fluctuations—not being affected by mean biases—and was thus directly computed.

The storage term in Equation 1 was computed from the slope of a linear fit of the scalar variance $\overline{s'^2}$ over 30 min. To compute the vertical derivatives for transport, we first fit a second order polynomial function across all four levels of the third order moments $\overline{w's's'}$; the derivative was then obtained from the slope of the respective polynomials for each period at $z = 3$ m. The dissipation of variance was estimated from the second-order structure function D_{ss} following Chamecki and Dias (2004) (more details in Section S2 in Supporting Information S1). Finally, while there are multiple variants of REA, depending on sensor response time and approaches to accumulate the fluxes (Foken, 2017), here we will only test that basic formulation where the s^+ and s^- are computed from high frequency data to simulate an actual REA system. We thus compute the term Δs by conditionally sampling s based on the sign of w' with no lower threshold on $|w'|$.

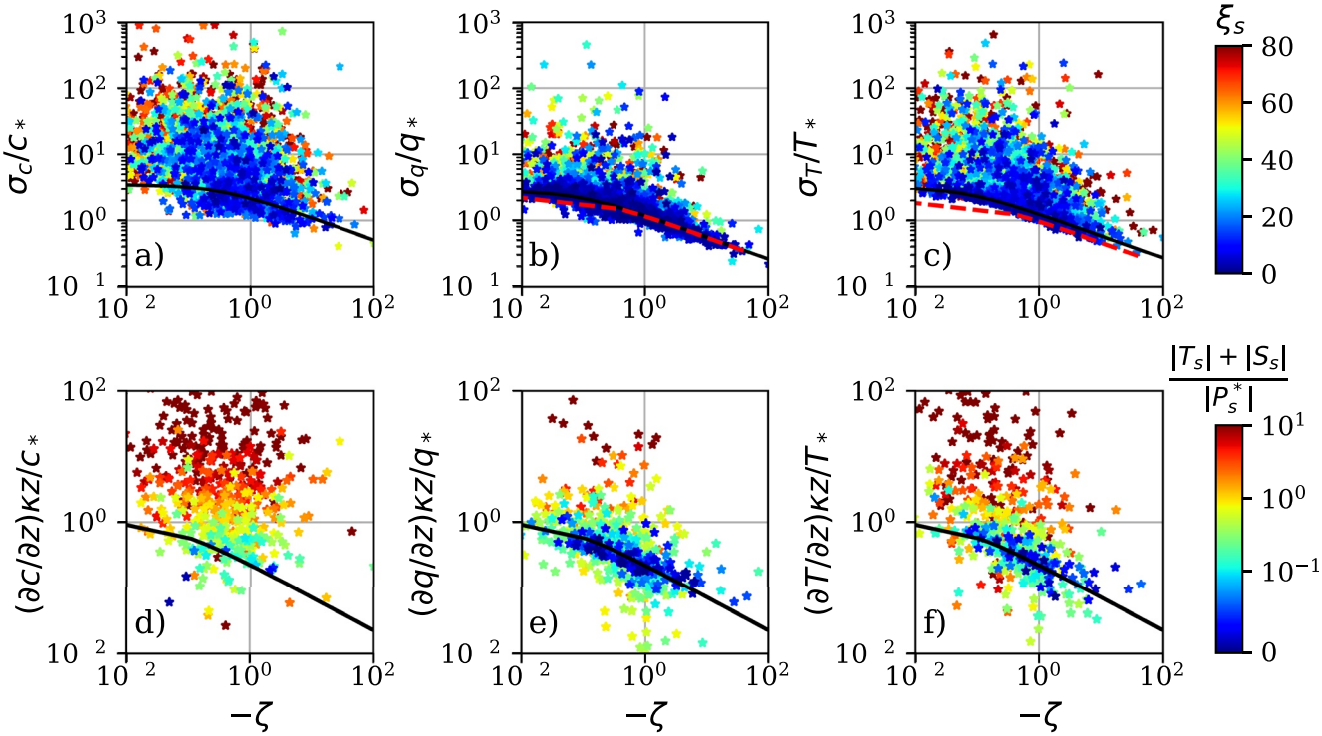

Figure 1. Variance function for (a) CO_2, (b) water vapor, and (c) temperature. Data for all four levels are included. The solid black line represents the empirical fit obtained over the lake using only "ideal" periods. Empirical curves found over homogeneous sites by Liu et al. (1998) are also shown in red. The color scheme represents the stationarity statistic. Flux-gradient function obtained from the residual of the variance budget Equation 1 for (d) CO_2, (e) water vapor, and (f) temperature. The color scheme represents the combined effects of nondimensional transport and storage terms. The empirical curve is from the large eddy simulation results of Maronga and Reuder (2017), with $C_1 = 1$ and $C_2 = 19.7$.

4. Results and Discussion

We first compute the variance function for all three scalars as shown in Figures 1a–1c, where we include the best fit for the empirical form as defined by Equation 7 (the color scheme represents the stationarity statistic from Equation 11). In the curve fitting process, we only considered data points where production and dissipation were in near balance to guarantee optimal MOST applicability as we will discuss in Section 4.1. Thus, by visual inspection of Figure 2, we selected only periods when transport and storage are negligible using the following criteria: $|S_s/P_s^*| < 0.1$ and $|T_s/P_s^*| < 1$ for CO_2, and $|S_s/P_s^*| < 0.01$ and $|T_s/P_c^*| < 0.5$ for water vapor and temperature, resulting in the following

$$\phi_c(\zeta) = 2.35(0.31 - \zeta)^{-1/3}, \tag{12}$$

$$\phi_q(\zeta) = 1.22(0.08 - \zeta)^{-1/3}, \tag{13}$$

$$\phi_T(\zeta) = 1.27(0.06 - \zeta)^{-1/3}. \tag{14}$$

Empirical curves obtained over a homogeneous surface by Liu et al. (1998) are shown in the figure, indicating a close agreement with the curves found over our lake.

Clearly, CO_2 has the most noticeable scatter, i.e., deviation from the MOST variance function even after filtering out periods most affected by storage and transport. Water vapor and temperature, on the other hand, are more similar (with closer fitting coefficients) when only "good" periods are retained (i.e., steady periods with small transport terms). In terms of stability, more deviation from MOST is observed for mildly unstable conditions ($\zeta \approx -0.1$). Notice that steady periods ($\xi_s < 30\%$) usually correspond to points close to the empirical curves, meaning that they are more likely to follow the scaling. Nonetheless, the presence of stationary periods that deviate from the expected values indicate that steadiness alone does not guarantee agreement with MOST. To further identify other causes for the deviation from MOST, we will now explore its connection to the variance budget.

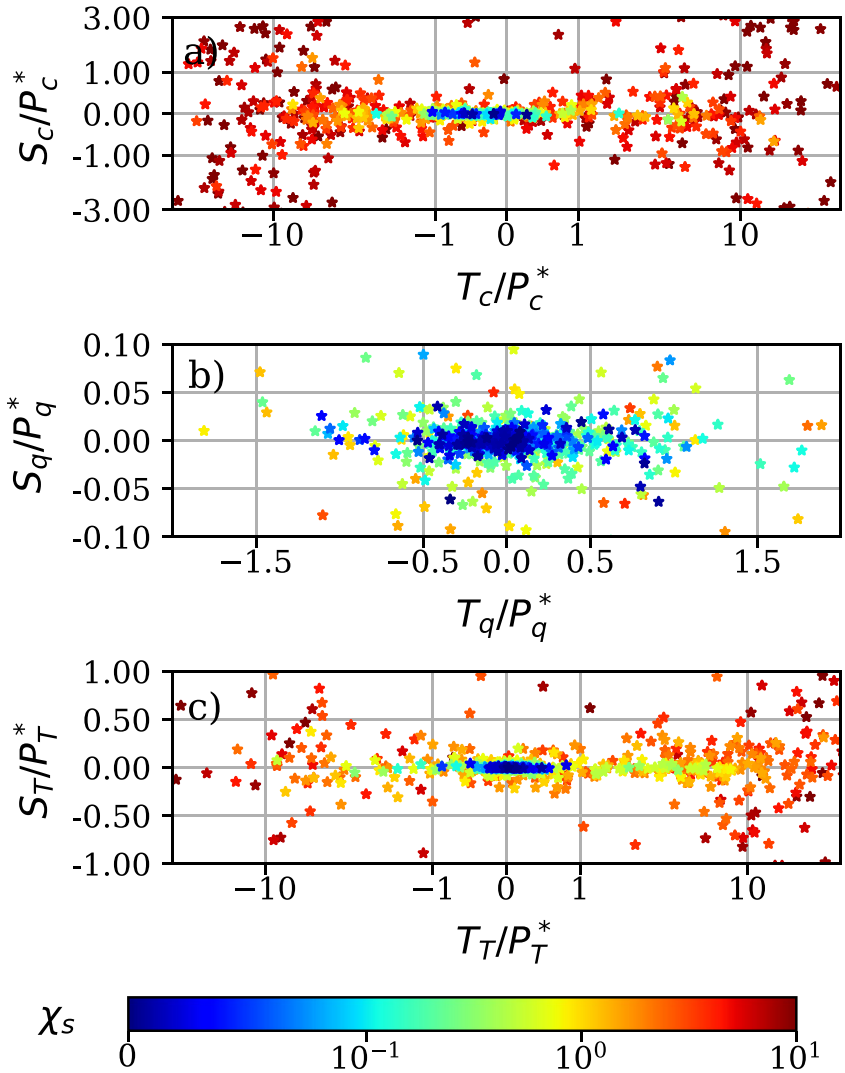

Figure 2. Storage versus transport terms of the variance budget for (a) CO_2, (b) water vapor, and (c) temperature. Color scheme represents the deviation from the empirical Monin-Obukhov Similarity Theory variance function as defined in Equation 15. $\chi_s > 10$ is represented in the darkest shade of red.

4.1. Deviation From the Variance Function Explained by the Budget Terms

To better compare departures from MOST across scalars and conditions and the potential role of various variance budget terms, we first define the metric χ_s,

$$\chi_s = \left| \frac{\phi_s(\zeta) - \sigma_s / s_*}{\phi_s(\zeta)} \right|. \tag{15}$$

As a reference, we chose ϕ_s obtained for water vapor over the lake, shown in Figure 1b, given its closer proximity to results obtained by Liu et al. (1998). In addition, because we computed the transport term at $z = 3$ m, we focus subsequent analyses on χ_s as measured by the third sensor (at $z = 2.95$ m).

The impact of the transport and storage terms on MOST is depicted in Figures 2a–2c, where the color scheme represents χ_s. Their dependence on stability is shown in Figure S2 in Supporting Information S1. Clearly, large transport values are associated with large deviation from MOST. In addition, large storage values also seem to cause large deviations from the theory. Note that transport and storage are slightly correlated (more obvious for CO_2), where large transport can be associated with large storage. Overall, the smallest deviations are observed when both terms are small compared to production. This result reveals that transport and storage are important in

practice for the applicability of MOST, and they can independently cause large deviations from the theory. These findings corroborate the hypothesis proposed by Cancelli et al. (2012) that both terms could play an important role in the failure of MOST.

4.2. Implications for the Flux-Gradient Method

Figures 1d–1f shows the performance of the flux-gradient function. As expected, more scatter is observed for CO_2 and temperature. Better agreement with the empirical fit is seen for water vapor, where points that deviate more are periods featuring large transport or storage of variance. Overall, we notice a similarity between the variance function and the gradient-flux methods in terms of how they are affected by variance storage and transport. This similarity can be explained by the variance budget itself. By combining a standard dissipation model $\epsilon_s = (C_\epsilon/\tau)\sigma_s^2$ (where C_ϵ is a similarity constant and τ a variance cascade time scale related to eddy turnover time) with the variance budget equation and expressions 2, 4, and 5, and ignoring the transport and storage terms, we can show that

$$\Psi_s(\zeta) = -C_\epsilon \frac{\kappa z}{u_* \tau} \phi_s^2(\zeta). \tag{16}$$

This equation shows that the flux-gradient and flux-variance methods are directly related. Furthermore, since $\kappa z/u_*$ is itself a reasonable estimate for the eddy turnover time, we expect $(\kappa z)/(u_*\tau) \simeq 1$. Thus, any disturbances to the variance function caused by storage or transport (or horizontal advection over other surfaces) also affect the FG (and vice-versa). Indeed, we found high correlation between the variance transport and flux transport ($w'w's'$, not shown here), which is aligned with earlier work documenting the role of the flux transport term in the breakdown of MOST (Raupach, 1979; Simpson et al., 1998).

4.3. Computing Fluxes With the Variance Function

The fluxes for all three scalars computed from the MOST variance-function method are compared to the eddy-covariance fluxes in Figures 3a–3c. As expected, fluxes computed from the theory are closer to the real measurements only when the combined transport and storage terms are small. In addition, the greatest errors tend to occur when the measured fluxes are small and are then widely overpredicted by MOST, which is associated with a weak local production term. On the other hand, stronger measured fluxes lead to a strong local production, which is then balanced by dissipation. These results are in agreement with the result of Cancelli et al. (2012) and Dias and Vissotto (2017) for fluxes over a lake in Brazil.

The poor results found for CO_2 are a consequence of the weak local production caused by the small fluxes from the lake. This result has direct implications for the exchanges of CO_2 and other trace gases between water and the atmosphere: if their fluxes are small, such that the equilibrium between production and dissipation of variance are disturbed, estimates obtained by MOST are less reliable (as also documented by De Bruin et al. (1999)). Therefore, these results indicate that alternative approaches to estimate fluxes in such situations are needed.

4.4. Performance of the Relaxed Eddy Accumulation Technique for Flux Estimation

As an alternative method to compute turbulent fluxes, we now investigate the REA method. We first computed the similarity coefficient β_s by inverting Equation 10. Negative coefficients were discarded, as well as $\beta_s > 1$. For all three scalars, we found the respective median and median absolute deviation to be 0.58 ± 0.10 (CO_2), 0.60 ± 0.03 (water vapor), and 0.58 ± 0.05 (temperature), in the range found by other authors (Businger & Oncley, 1990; Katul, Finkelstein, et al., 1996; Sakabe et al., 2014; Vogl et al., 2021; Zahn, Dias, et al., 2016). This variability in β_c of around 20% from its median (Figures S3 and S4 in Supporting Information S1) is much smaller compared to the scatter seen for the variance function (Figure 1a), which can be up to three orders of magnitude above the value predicted by MOST.

To investigate the weak dependence of β_s on stability, we rewrite the REA equation as

$$\frac{1}{\beta_s} = \frac{\sigma_w \Delta_s}{\overline{w's'}} = \frac{\sigma_w}{u_*} \frac{\Delta s}{s_*} = \phi_w(\zeta)\eta_s(\zeta), \tag{17}$$

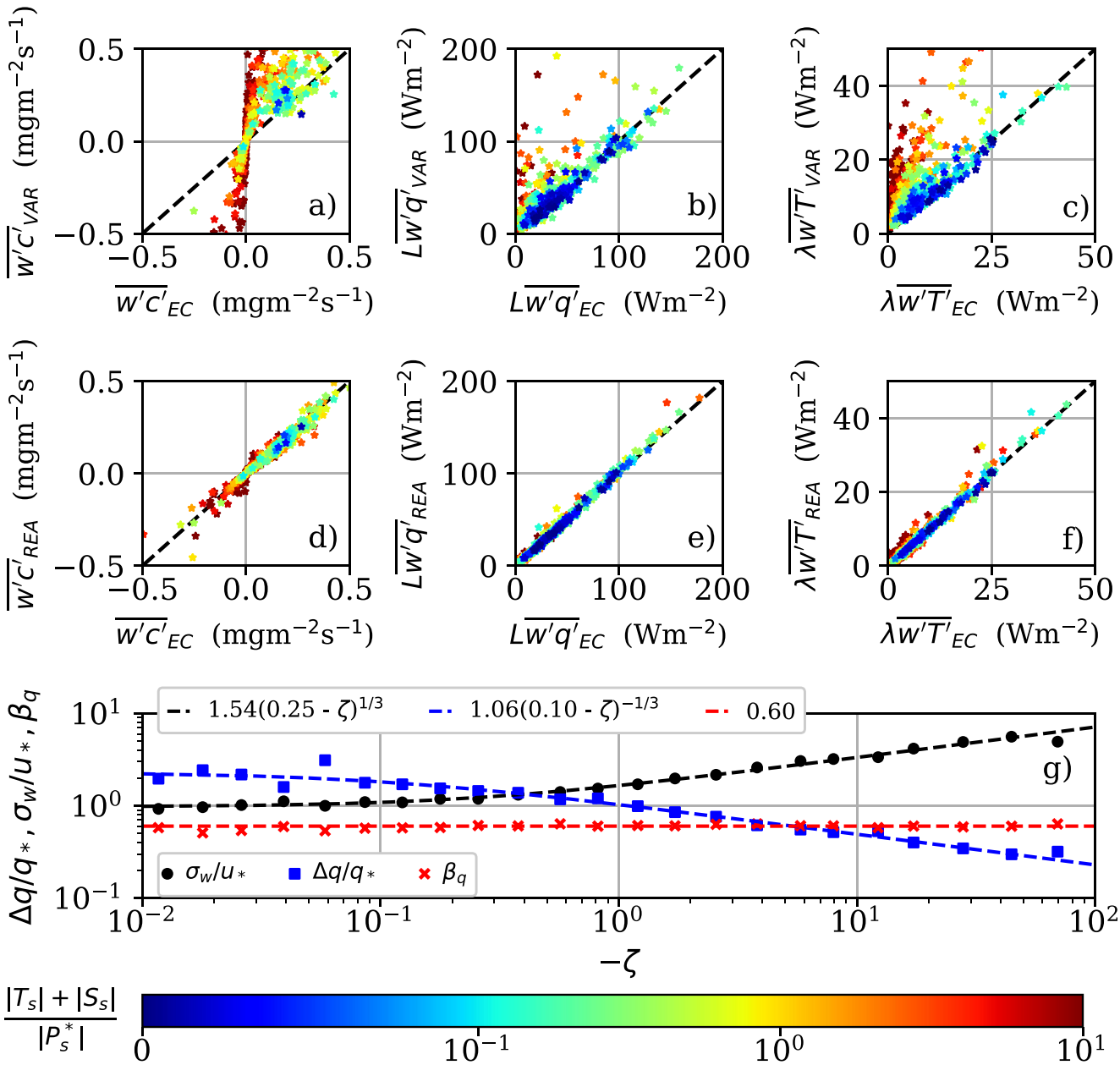

Figure 3. Comparison of eddy covariance fluxes $\left(\overline{w's'}_{EC}\right)$ versus flux estimated by the variance-flux method for (a) CO_2, (b) water vapor, and (c) temperature, and versus fluxes estimated by relaxed eddy accumulation for (d) CO_2, (e) water vapor, and (f) temperature. L and λ are factors converting the kinematic fluxes to latent and sensible heat flux, respectively. Subplot (g) shows bin averages of $\Delta q/q_*$, σ_w/u_*, and β_q versus stability.

where we postulate that $\eta_s = \Delta s/s_*$ is a function of stability. The bin averages of ϕ_w and η_q are shown in Figure 3g, where we can see a clear dependence on ζ (detailed results for all three scalars are included in Section S4 in Supporting Information S1). The same figure, on the other hand, shows that β_q is constant. But rather than being a fortuitous or empirical result, the figure and Equation 17 demonstrate that the independence of β_q from stability is the result of the exact cancellation of the ζ effects in the multiplication between $\phi_w \propto \zeta^{1/3}$ and $\eta_q \propto \zeta^{-1/3}$. Since both of these exponents are derived to ensure independence from u_* in the free convection limit, the scaling $\beta \propto \zeta^0$ is itself a requirement if REA is to recover that free convection scaling. This result thus explains the weak or non existent dependence of β_s on ζ—at least under unstable conditions—found but not explained in previous studies (Baker et al., 1992; Katul, Finkelstein, et al., 1996; Zahn, Dias, et al., 2016), and confirms Foken's hypothesis who suggested that the weak dependence was likely caused by the canceling effects of stability (Foken, 2017, p. 184).

We thus find it practical and reasonable to set a constant $\beta_s = 0.59$ for all scalars, which also better mimics a field experiment where no proxy scalars are available.

Figures 3d–3f compares the eddy-covariance fluxes to the fluxes computed by the REA for all scalars. Noticeably, a much better agreement is obtained, in particular for small flux magnitudes. Good agreement between REA and EC estimates has previously been observed for CO_2 over a soybean field (Pattey et al., 1993), wheat and barley crops (Gallagher et al., 2000), a coniferous forest (Hamotani et al., 1996), and wetlands (Tsai et al., 2012), as well as for isoprene over a mixed forest (Bowling et al., 1998). Thus, we further confirm the advantages of REA as a flux estimation method over MOST-based models. In particular, the REA is more robust to the influence of variance storage and transport. This results from the main assumption underlying its derivation, which only requires linearity between w' and s'. Thus, as long as their linearity is not strongly impacted by transport and storage, fluxes estimated by the REA should be very close to their eddy-covariance counterparts (Katul et al., 2018). Further discussion of the robustness of the REA method is included Sections S1 (see Figure S1 in Supporting Information S1), S4 and S5 (see Figure S5 in Supporting Information S1).

The insensitivity of REA to the production-dissipation equilibrium, which is the exception rather than the rule in many field experiment conditions, thus emerges as a substantial practical advantage. Therefore, our findings support the implementation of the REA method, as opposed to MOST, to estimate small flux magnitudes. Nonetheless, we note that there are still practical challenges concerning accurate measurements of trace gases and implementation of the REA. This has led to modifications of the method aiming at removing noisy measurements by restricting the sampling of updrafts and downdrafts based on a minimum magnitude of the vertical velocity (Businger & Oncley, 1990; Pattey et al., 1993; Vogl et al., 2021). In this paper, however, we mainly focused on the theoretical basis of the method, ignoring other practical aspects related to sensor sensitivity and accumulation device design, among others.

5. Conclusion

Our findings confirm that MOST's performance hinges on the assumption of local equilibrium between variance production and dissipation. In other words, any disruption of this equilibrium, such as storage and transport, might lead to departure from the theory and flux overestimation. Small flux magnitudes are usually in non-equilibrium, and thus are more likely to be misrepresented by MOST. As a consequence, MOST's application is somewhat limited to strong flux conditions (note that the definition of “weak” and “strong” fluxes depend on the scalar in question). However, since MOST overestimates the eddy-covariance measured fluxes, it may not be possible in practice to identify low flux period using MOST itself to avoid large errors.

On the other hand, REA's performance does not rely on local equilibrium, being capable of estimating reliable fluxes even under non-ideal conditions. Therefore, REA is a valuable tool for trace-gas flux estimation that should be more broadly adopted in field experiments when possible, particularly that our study demonstrates why the REA coefficient β is required to be independent of stability. However, an alternative to MOST in the land-surface parameterizations of Earth-System models, where REA is not a suitable alternative, remains elusive.

Data Availability Statement

The raw eddy-covariance data used for analyses in the study are available at https://doi.org/10.5281/zenodo.7591387 (Zahn, 2023a). The processed data used to reproduce all figures are available at https://doi.org/10.5281/zenodo.7591524 (Zahn, 2023b).

Acknowledgments
EZ and EBZ are supported by the US National Science Foundation under award number AGS 2128345 and EAR 2126206 and by the Cooperative Institute for Modeling the Earth System at Princeton University under Award NA18OAR4320123 from the National Oceanic and Atmospheric Administration. This material is based upon work supported by the High Meadows Environmental Institute at Princeton University through the Walbridge Fund Graduate Award for Environmental Research. The authors would also like to thank Gabriel G. Katul for his insight on the derivations in Section S1 in Supporting Information S1.

References

Armani, F. A. S., Dias, N. L., & Vissotto Junior, D. (2020). Similarity between turbulent fluctuations of scalars in lake environment. *Ciencia e Natura*, *42*, e13. https://doi.org/10.5902/2179460X45355

Asanuma, J., & Brutsaert, W. (1999). Turbulence variance characteristics of temperature and humidity in the unstable atmospheric surface layer above a variable pine forest. *Water Resources Research*, *35*(2), 515–521. https://doi.org/10.1029/1998WR900051

Assouline, S., Tyler, S., Tanny, J., Cohen, S., Bou-Zeid, E., Parlange, M., & Katul, G. (2008). Evaporation from three water bodies of different sizes and climates: Measurements and scaling analysis. *Advances in Water Resources*, *31*(1), 160–172. https://doi.org/10.1016/j.advwatres.2007.07.003

Baker, J., Norman, J., & Bland, W. (1992). Field-scale application of flux measurement by conditional sampling. *Agricultural and Forest Meteorology*, *62*(1–2), 31–52. https://doi.org/10.1016/0168-1923(92)90004-n

Barskov, K., Stepanenko, V., Repina, I., Artamonov, A., & Gavrikov, A. (2019). Two regimes of turbulent fluxes above a frozen small lake surrounded by forest. *Boundary-Layer Meteorology*, *173*(3), 311–320. https://doi.org/10.1007/s10546-019-00469-w

Bou-Zeid, E., Vercauteren, N., Parlange, M. B., & Meneveau, C. (2008). Scale dependence of subgrid-scale model coefficients: An a priori study. *Physics of Fluids*, *20*(11), 115106. https://doi.org/10.1063/1.2992192

Bowling, D. R., Turnipseed, A., Delany, A., Baldocchi, D., Greenberg, J., & Monson, R. (1998). The use of relaxed eddy accumulation to measure biosphere-atmosphere exchange of isoprene and other biological trace gases. *Oecologia*, *116*(3), 306–315. https://doi.org/10.1007/s004420050592

Businger, J. A., & Oncley, S. P. (1990). Flux measurement with conditional sampling. *Journal of Atmospheric and Oceanic Technology*, *7*(2), 349–352. https://doi.org/10.1175/1520-0426(1990)007⟨0349:FMWCS⟩2.0.CO;2

Businger, J. A., Wyngaard, J. C., Izumi, Y., & Bradley, E. F. (1971). Flux-profile relationships in the atmospheric surface layer. *Journal of the Atmospheric Sciences*, *28*(2), 181–189. https://doi.org/10.1175/1520-0469(1971)028⟨0181:FPRITA⟩2.0.CO;2

Cancelli, D. M., Dias, N. L., & Chamecki, M. (2012). Dimensionless criteria for the production-dissipation equilibrium of scalar fluctuations and their implications for scalar similarity. *Water Resources Research*, *48*(10), W10522. https://doi.org/10.1029/2012WR012127

Cava, D., Katul, G. G., Sempreviva, A., Giostra, U., & Scrimieri, A. (2008). On the anomalous behaviour of scalar flux-variance similarity functions within the canopy sub-layer of a dense alpine forest. *Boundary-Layer Meteorology*, *128*(1), 33–57. https://doi.org/10.1007/s10546-008-9276-z

Chamecki, M., & Dias, N. L. (2004). The local isotropy hypothesis and the turbulent kinetic energy dissipation rate in the atmospheric surface layer. *Quarterly Journal of the Royal Meteorological Society*, *130*(603), 2733–2752. https://doi.org/10.1256/qj.03.155

Chor, T. L., Dias, N. L., Araújo, A., Wolff, S., Zahn, E., Manzi, A., et al. (2017). Flux-variance and flux-gradient relationships in the roughness sublayer over the amazon forest. *Agricultural and Forest Meteorology*, *239*, 213–222. https://doi.org/10.1016/j.agrformet.2017.03.009

De Bruin, H., Kohsiek, W., & Van Den Hurk, B. (1993). A verification of some methods to determine the fluxes of momentum, sensible heat, and water vapour using standard deviation and structure parameter of scalar meteorological quantities. *Boundary-Layer Meteorology*, *63*(3), 231–257. https://doi.org/10.1007/BF00710461

De Bruin, H., Van Den Hurk, B., & Kroon, L. (1999). On the temperature-humidity correlation and similarity. *Boundary-Layer Meteorology*, *93*(3), 453–468. https://doi.org/10.1023/A:1002071607796

Dellwik, E., & Jensen, N. O. (2005). Flux–profile relationships over a fetch limited beech forest. *Boundary-Layer Meteorology*, *115*(2), 179–204. https://doi.org/10.1007/s10546-004-3808-y

Denmead, O. T., & Bradley, E. F. (1985). Flux-gradient relationships in a forest canopy. In B. A. Hutchison & B. B. Hicks (Eds.), *The forest-atmosphere interaction: Proceedings of the forest environmental measurements conference held at oak ridge, Tennessee* (pp. 421–442). Springer Netherlands. https://doi.org/10.1007/978-94-009-5305-5_27

Detto, M., Katul, G., Mancini, M., Montaldo, N., & Albertson, J. (2008). Surface heterogeneity and its signature in higher-order scalar similarity relationships. *Agricultural and Forest Meteorology*, *148*(6–7), 902–916. https://doi.org/10.1016/j.agrformet.2007.12.008

Detto, M., & Katul, G. G. (2007). Simplified expressions for adjusting higher-order turbulent statistics obtained from open path gas analyzers. *Boundary-Layer Meteorology*, *122*(1), 1573–1472. https://doi.org/10.1007/s10546-006-9105-1

Dias, N. L., Hong, J., Leclerc, M. Y., Black, T. A., Nesic, Z., & Krishnan, P. (2009). A simple method of estimating scalar fluxes over forests. *Boundary-Layer Meteorology*, *132*(3), 401–414. https://doi.org/10.1007/s10546-009-9408-0

Dias, N. L., & Vissotto, D., Jr. (2017). The effect of temperature-humidity similarity on Bowen ratios, dimensionless standard deviations, and mass transfer coefficients over a lake. *Hydrological Processes*, *31*(2), 256–269. https://doi.org/10.1002/hyp.10925

Dyer, A. J. (1974). A review of flux-profile relationships. *Boundary-Layer Meteorology*, *7*(3), 363–372. https://doi.org/10.1007/BF00240838

Dyer, A. J., & Hicks, B. B. (1970). Flux-gradient relationships in the constant flux layer. *Quarterly Journal of the Royal Meteorological Society*, *96*(410), 715–721. https://doi.org/10.1002/qj.49709641012

Foken, T. (2006). 50 years of the Monin–Obukhov similarity theory. *Boundary-Layer Meteorology*, *119*(3), 431–447. https://doi.org/10.1007/s10546-006-9048-6

Foken, T. (2017). *Micrometeorology* (pp. 175–176). Springer Berlin. https://doi.org/10.1007/978-3-642-25440-6

Gallagher, M., Clayborough, R., Beswick, K., Hewitt, C., Owen, S., Moncrieff, J., & Pilegaard, K. (2000). Assessment of a relaxed eddy accumulation for measurements of fluxes of biogenic volatile organic compounds: Study over arable crops and a mature beech forest. *Atmospheric Environment*, *34*(18), 2887–2899. https://doi.org/10.1016/S1352-2310(00)00066-2

Hamotani, K., Uchida, Y., Monji, N., & Miyata, A. (1996). A system of the relaxed eddy accumulation method to evaluate CO_2 flux over plant canopies. *Journal of Agricultural Meteorology*, *52*(2), 135–139. https://doi.org/10.2480/agrmet.52.135

Hill, R. J. (1989). Implications of Monin–Obukhov similarity theory for scalar quantities. *Journal of the Atmospheric Sciences*, *46*(14), 2236–2244. https://doi.org/10.1175/1520-0469(1989)046⟨2236:IOMSTF⟩2.0.CO;2

Hogstrom, U. (1988). Non-dimensional wind and temperature profiles in the atmospheric surface layer: A re-evaluation. *Boundary-Layer Meteorology*, *42*(1–2), 55–78. https://doi.org/10.1007/BF00119875

Hsieh, C.-I., Lai, M.-C., Hsia, Y.-J., & Chang, T.-J. (2008). Estimation of sensible heat, water vapor, and CO_2 fluxes using the flux-variance method. *International Journal of Biometeorology*, *52*(6), 521–533. https://doi.org/10.1007/s00484-008-0149-4

Iwata, T., Yoshikawa, K., Nishimura, K., Higuchi, Y., Yamashita, T., Kato, S., & Ohtaki, E. (2004). CO_2 flux measurements over the sea surface by eddy correlation and aerodynamic techniques. *Journal of Oceanography*, *60*(6), 995–1000. https://doi.org/10.1007/s10872-005-0007-5

Kaimal, J. C., & Finnigan, J. J. (1994). *Atmospheric boundary layer flows: Their structure and measurement*. Oxford University Press. https://doi.org/10.1007/BF00712396

Katul, G. G., Albertson, J., Chu, C.-R., Parlange, M., Stricker, H., & Tyler, S. (1994). Sensible and latent heat flux predictions using conditional sampling methods. *Water Resources Research*, *30*(11), 3053–3059. https://doi.org/10.1029/94wr01673

Katul, G. G., Goltz, S. M., Hsieh, C.-I., Cheng, Y., Mowry, F., & Sigmon, J. (1995). Estimation of surface heat and momentum fluxes using the flux-variance method above uniform and non-uniform terrain. *Boundary-Layer Meteorology*, *74*(3), 237–260. https://doi.org/10.1007/BF00712120

Katul, G. G., Hsieh, C.-I., Oren, R., Ellsworth, D., & Phillips, N. (1996). Latent and sensible heat flux predictions from a uniform pine forest using surface renewal and flux variance methods. *Boundary-Layer Meteorology*, *80*(3), 249–282. https://doi.org/10.1007/bf00119545

Katul, G. G., Peltola, O., Grönholm, T., Launiainen, S., Mammarella, I., & Vesala, T. (2018). Ejective and sweeping motions above a peatland and their role in relaxed-eddy-accumulation measurements and turbulent transport modelling. *Boundary-Layer Meteorology*, *169*(2), 163–184. https://doi.org/10.1007/s10546-018-0372-4

Lammert, A., & Ament, F. (2015). CO_2-flux measurements above the Baltic sea at two heights: Flux gradients in the surface layer? *Earth System Science Data*, *7*(2), 311–317. https://doi.org/10.5194/essd-7-311-2015

Li, D., Bou-Zeid, E., & De Bruin, H. A. R. (2012). Monin–Obukhov similarity functions for the structure parameters of temperature and humidity. *Boundary-Layer Meteorology*, *145*(1), 45–67. https://doi.org/10.1007/s10546-011-9660-y

Liu, X., Tsukamoto, O., Oikawa, T., & Ohtaki, E. (1998). A study of correlations of scalar quantities in the atmospheric surface layer. *Boundary-Layer Meteorology*, *87*(3), 499–508. https://doi.org/10.1023/A:1000947709324

Maronga, B., & Reuder, J. (2017). On the formulation and universality of Monin–Obukhov similarity functions for mean gradients and standard deviations in the unstable surface layer: Results from surface-layer-resolving large-eddy simulations. *Journal of the Atmospheric Sciences*, *74*(4), 989–1010. https://doi.org/10.1175/JAS-D-16-0186.1

Monin, A., & Obukhov, A. (1954). Basic laws of turbulent mixing in the surface layer of the atmosphere. *Contrib. Geophys. Inst. Acad. Sci. USSR*, *24*, 163–187.

Pattey, E., Desjardins, R. L., & Rochette, P. (1993). Accuracy of the relaxed eddy-accumulation technique, evaluated using CO_2 flux measurements. *Boundary-Layer Meteorology*, *66*(4), 341–355. https://doi.org/10.1007/BF00712728

Raupach, M. (1979). Anomalies in flux-gradient relationships over forest. *Boundary-Layer Meteorology*, *16*(3), 467–486. https://doi.org/10.1007/BF03335385

Sakabe, A., Ueyama, M., Kosugi, Y., Hamotani, K., Hirano, T., & Hirata, R. (2014). Is the empirical coefficient b for the relaxed eddy accumulation method constant? *Journal of Atmospheric Chemistry*, *71*(1), 79–94. https://doi.org/10.1007/s10874-014-9282-0

Simpson, I. J., Thurtell, G. W., Neumann, H. H., Den Hartog, G., & Edwards, G. C. (1998). The validity of similarity theory in the roughness sublayer above forests. *Boundary-Layer Meteorology*, *87*(1), 1573–1472. https://doi.org/10.1023/A:1000809902980

Stull, R. B. (1988). *An introduction to boundary layer meteorology*. Springer. https://doi.org/10.1007/978-94-009-3027-8

Tsai, J.-L., Tsuang, B.-J., Kuo, P.-H., Tu, C.-Y., Chen, C.-L., Hsueh, M.-T., et al. (2012). Evaluation of the relaxed eddy accumulation coefficient at various wetland ecosystems. *Atmospheric Environment*, *60*, 336–347. https://doi.org/10.1016/j.atmosenv.2012.06.081

Vercauteren, N., Bou-Zeid, E., Parlange, M. B., Lemmin, U., Huwald, H., Selker, J., & Meneveau, C. (2008). Subgrid-scale dynamics of water vapour, heat, and momentum over a lake. *Boundary-Layer Meteorology*, *128*(2), 205–228. https://doi.org/10.1007/s10546-008-9287-9

Vogl, T., Hrdina, A., & Thomas, C. K. (2021). Choosing an optimal β factor for relaxed eddy accumulation applications across vegetated and non-vegetated surfaces. *Biogeosciences*, *18*(18), 5097–5115. https://doi.org/10.5194/bg-18-5097-2021

Waterman, T., Bragg, A. D., Katul, G., & Chaney, N. (2022). Examining parameterizations of potential temperature variance across varied landscapes for use in Earth system models. *Journal of Geophysical Research: Atmospheres*, *127*(8), e2021JD036236. https://doi.org/10.1029/2021JD036236

Weaver, H. L. (1990). Temperature and humidity flux-variance relations determined by one-dimensional eddy correlation. *Boundary-Layer Meteorology*, *53*(1–2), 77–91. https://doi.org/10.1007/BF00122464

Williams, C. A., Scanlon, T. M., & Albertson, J. D. (2007). Influence of surface heterogeneity on scalar dissimilarity in the roughness sublayer. *Boundary-Layer Meteorology*, *122*(1), 149–165. https://doi.org/10.1007/s10546-006-9097-x

Wyngaard, J. C., Coté, O. R., & Izumi, Y. (1971). Local free convection, similarity, and the budgets of shear stress and heat flux. *Journal of the Atmospheric Sciences*, *28*(7), 1171–1182. https://doi.org/10.1175/1520-0469(1971)028⟨1171:LFCSAT⟩2.0.CO;2

Xiao, W., Liu, S., Li, H., Xiao, Q., Wang, W., Hu, Z., et al. (2014). A flux-gradient system for simultaneous measurement of the CH_4, CO_2, and H_2O fluxes at a lake–air interface. *Environmental Science & Technology*, *48*(24), 14490–14498. https://doi.org/10.1021/es5033713

Zahn, E. (2023a). Raw Eddy-Covariance data (Version 1) [Dataset]. Zenodo. https://doi.org/10.5281/zenodo.7591387

Zahn, E. (2023b). Processed Data MOST (Version 1) [Dataset]. Zenodo. https://doi.org/10.5281/zenodo.7591524

Zahn, E., Chor, T. L., & Dias, N. L. (2016). A simple methodology for quality control of micrometeorological datasets. *American Journal of Environmental Engineering*, *6*(4A), 135–142. https://doi.org/10.5923/s.ajee.201601.20

Zahn, E., Dias, N. L., Araújo, A., Sá, L. D. A., Sörgel, M., Trebs, I., et al. (2016). Scalar turbulent behavior in the roughness sublayer of an Amazonian forest. *Atmospheric Chemistry and Physics*, *16*(17), 11349–11366. https://doi.org/10.5194/acp-16-11349-2016

Zemmelink, H. J., Dacey, J. W., & Hintsa, E. J. (2004). Direct measurements of biogenic dimethylsulphide fluxes from the oceans: A synthesis. *Canadian Journal of Fisheries and Aquatic Sciences*, *61*(5), 836–844. https://doi.org/10.1139/f04-047

Zhao, J., Zhang, M., Xiao, W., Wang, W., Zhang, Z., Yu, Z., et al. (2019). An evaluation of the flux-gradient and the eddy covariance method to measure CH_4, CO_2, and H_2O fluxes from small ponds. *Agricultural and Forest Meteorology*, *275*, 255–264. https://doi.org/10.1016/j.agrformet.2019.05.032

References From the Supporting Information

Allouche, M., Bou-Zeid, E., Ansorge, C., Katul, G. G., Chamecki, M., Acevedo, O., et al. (2022). The detection, genesis, and modeling of turbulence intermittency in the stable atmospheric surface layer. *Journal of the Atmospheric Sciences*, *79*(4), 1171–1190. https://doi.org/10.1175/JAS-D-21-0053.1

Bou-Zeid, E., Higgins, C., Huwald, H., Meneveau, C., & Parlange, M. B. (2010). Field study of the dynamics and modelling of subgrid-scale turbulence in a stable atmospheric surface layer over a glacier. *Journal of Fluid Mechanics*, *665*, 480–515. https://doi.org/10.1017/S0022112010004015

Katul, G. G., Finkelstein, P. L., Clarke, J. F., & Ellestad, T. G. (1996). An investigation of the conditional sampling method used to estimate fluxes of active, reactive, and passive scalars. *Journal of Applied Meteorology and Climatology*, *35*(10), 1835–1845. https://doi.org/10.1175/1520-0450(1996)035<1835:aiotcs>2.0.co;2

Milne, R., Beverland, I. J., Hargreaves, K., & Moncrieff, J. B. (1999). Variation of the β coefficient in the relaxed eddy accumulation method. *Boundary-Layer Meteorology*, *93*(2), 211–225. https://doi.org/10.1023/A:1002061514948